Breast Cancer Res Treat
DOI 10.1007/s10549-010-0884-1

PRECLINICAL STUDY

Uptake of 2-NBDG as a method to monitor therapy response in breast cancer cell lines

Stacy R. Millon · Julie H. Ostrander · J. Quincy Brown · Anita Raheja · Victoria L. Seewaldt · Nirmala Ramanujam

Received: 25 January 2010 / Accepted: 1 April 2010

Abstract This study quantifies uptake of a fluorescent glucose analog, (2-(*N*-(7-nitrobenz-2-oxa-1,3-diazol-4-yl)amino)-2-deoxyglucose) (2-NBDG), in a large panel of breast cancer cells and demonstrates potential to monitor changes in glycolysis caused by anticancer and endocrine therapies. Expressions of glucose transporter (GLUT 1) and hexokinase (HK I), which phosphorylates 2-NBDG, were measured via western blot in two normal mammary epithelial and eight breast cancer cell lines of varying biological subtype. Fluorescence intensity of each cell line labeled with 100 μM 2-NBDG for 20 min or unlabeled control was quantified. A subset of cancer cells was treated with anticancer and endocrine therapies, and 2-NBDG fluorescence changes were measured. Expression of GLUT 1 was necessary for uptake of 2-NBDG, as demonstrated by lack of 2-NBDG uptake in normal human mammary epithelial cells (HMECs). GLUT 1 expression and 2-NBDG uptake was ubiquitous among all breast cancer lines. Reduction and stimulation of 2-NBDG uptake was demonstrated by perturbation with anticancer agents, lonidamine (LND), and α-cyano-hydroxycinnamate (α-Cinn), respectively. LND directly inhibits HK and significantly reduced 2-NBDG fluorescence in a subset of two breast cancer cell lines. Conversely, when cells were treated with α-Cinn, a drug used to increase glycolysis, 2-NBDG uptake was increased. Furthermore, tamoxifen (tam), a common endocrine therapy, was administered to estrogen receptor positive and negative (ER+/−) breast cells and demonstrated a decreased 2-NBDG uptake in ER+ cells, reflecting a decrease in glycolysis. Results indicate that 2-NBDG uptake can be used to measure changes in glycolysis and has potential for use in early drug development.

Keywords 2-NBDG · Breast cancer cell lines · Confocal microscopy · GLUT 1 · Tamoxifen

Introduction

Functional imaging of glucose uptake has been shown to be invaluable in breast cancer diagnosis, prognosis, and therapy monitoring [1]. Many cancers demonstrate aerobic glycolysis, glucose metabolism in the presence of oxygen [1–3]. Current methods to measure glycolysis include measurement of dielectric response [4], protein quantification [5], nuclear resonance and imaging [1, 6, 7], microarray quantification [8], and pH responsive dyes [9]. Monitoring glycolysis is most commonly measured with fluoro-deoxyglucose (FDG), a radioactive glucose analog, and is detected with Positron Emission Tomography (PET) [1]. All of these techniques, however, can be prohibitively expensive, manually intensive, and/or technologically complex rendering them impractical for high-throughput drug development even with demonstration of clinical success [1].

2-(*N*-(7-nitrobenz-2-oxa-1,3-diazol-4-yl)amino)-2-deoxyglucose (2-NBDG) is an optical contrast agent that follows a similar metabolic pathway to D-glucose [3]. 2-NBDG enters the cell via glucose transporters (GLUT), and is

S. R. Millon (✉) · J. Q. Brown · A. Raheja · N. Ramanujam
Department of Biomedical Engineering, Duke University, 136 Hudson Hall, Campus, Box 90281, Durham, NC 27708-0281, USA
e-mail: stacy.millon@duke.edu

J. H. Ostrander · V. L. Seewaldt
Department of Medicine, Duke University, Durham, NC, USA

Published online: 14 April 2010

phosphorylated at the C-6 position by hexokinases I–II (HK) [3]. The phosphorylated fluorescent metabolite 2-NBDG-6-phosphate remains in the cell until further decomposition occurs into a non-fluorescent form [10]. 2-NBDG can be maximally excited at 488 nm and emits at 540 nm. Cellular glycolysis and the proteins GLUT 1 and HK I have all previously been shown to be up regulated in breast cancer [11] and thus, it would be expected that increased glycolysis would lead to increased accumulation of 2-NBDG in malignant relative to benign tissues [2, 3].

Previous studies to examine applications of 2-NBDG have focused on cancer detection in vivo [12], on ex vivo tissue [2], or in vitro [3, 13]. Preferential accumulation of 2-NBDG in cancer tissue over surrounding normal tissue was demonstrated to be 3.7× higher in 20 neoplastic ex vivo oral biopsy specimens compared to matched normal tissue biopsies [2]. Sheth et al. demonstrated the pre-clinical utility of 2-NBDG in several in vivo mouse models, demonstrating 2-NBDG uptake was greater in a fasting (glucose deprived) animal compared to a non-fasting animal, was co-localized with RFP in a gliosarcoma tumor within a period of 60 min (Warburg Effect) and demonstrated preferential uptake in a stimulated seizure model of the brain as compared to one that was free of seizures [12].

Preferential uptake of 2-NBDG in breast cancer has been carried out previously on in vitro cell studies, but not in pre-clinical models of breast cancers or human breast cancers. O'Neil et al. demonstrated a 3.5× greater uptake of 2-NBDG in MCF7 cells as compared to non-malignant M-1 epithelial cells following 10 min of incubation in 0.3 mM concentration of the contrast agent [3]. Levi et al. used MCF7, MDA-MB-435, and MDA-MB-231 cell lines to compare 2-NBDG uptake at 10 μM to 10 μM of NIR-fructose uptake after 15 min of incubation and found them to be equivalent [13].

(2-(*N*-(7-nitrobenz-2-oxa-1,3-diazol-4-yl)amino)-2-deoxyglucose) could play an important role in in vitro cell line studies. 2-NBDG allows for the evaluation of the efficacy of drugs on a large number of different cell lines, which is particularly important given the heterogeneity of breast disease. The objective of the study reported here was to demonstrate the utility of 2-NBDG as a molecular contrast agent to quantitatively measure changes in glycolysis and to demonstrate a method to measure the response of breast cancer cell lines to therapy. Confocal microscopy was used to image the fluorescence signal from 2-NBDG in a panel of 10 different breast cell lines—two normal mammary epithelial and eight cancer that included estrogen receptor positive (ER+) and negative (ER−) cell lines. The expression of GLUT 1 and HK I proteins were quantified following western blot analysis and compared to fluorescence results obtained from these cells. A subset of two breast cancer cell lines was then treated with anticancer therapies that directly affect glycolysis: lonidamine (LND), a HK inhibitor, and α-cyano-hydroxycinnamate (α-Cinn), a glycolytic stimulator, to demonstrate the ability to measure opposing perturbations on 2-NBDG uptake. Finally, a subset of 1 ER+ and 1 ER− breast cancer cell lines was treated with a therapeutic dose of tamoxifen (tam), a widely used endocrine therapy for treatment of patients with ER+ breast cancer, to determine if the changes in 2-NBDG uptake are consistent with the expected effects of tam, a reduction in glycolysis.

Methods and materials

Cell culture

Two cell lines were derived from the normal mammary epithelium (MCF12 and human mammary epithelial cells (HMEC)), and eight were derived from patients with breast cancer (BT-20, BT-474, MDA-MB-231, MDA-MB-361, MDA-MB-435, MDA-MB-468, MCF7, and T47D). Breast cancer cell lines and the MCF12 cell line were obtained from the American Type Culture collection, ATCC (Manassas, VA, USA). Primary HMECs were obtained from Lonza (Basel, Switzerland) and infected with a retrovirus encoding human telomerase reverse transcriptase (hTERT) for immortalization. All cells remained free of contaminants and were propagated by adherent culture, trypsinized, and plated according to established protocols [14, 15]. Cells were plated at 100,000 cells/ml in 10 ml for western blot analysis and 2 ml for all confocal imaging studies.

Confocal microscopy parameters

All confocal images were collected on a Leica SP5 laser scanning confocal microscope (Wetzlar, Germany) using a previously published protocol [15]. Briefly, a 488-nm argon laser source (power at sample was 3.5 mW) was coupled to an inverted Leica DM16000CS microscope with a 40× oil-immersion objective (Leica Plan NeoFluor, NA = 1.25). Emission was collected at 515–585 nm, chosen from preliminary spectroscopy data on MCF7 cells to incorporate the full-width half-maximum of 2-NBDG. Images were acquired with a PMT gain of 950 V, offset 0.7%, and zoom of 1.6 to measure the unlabeled and labeled 2-NBDG cells. This gain was chosen for quantification of weakly fluorescent unlabeled cells to allow comparison to 2-NBDG-labeled cells. Images of anticancer and endocrine therapy treated and vehicle control cells (all 2-NBDG labeled) were acquired with a gain of 750 V, offset 0.7%, and zoom of 1.6. The gain was lowered since some 2-NBDG labeled cell lines had saturated pixels in the first set of experiments, specifically MDA-MB-435.

Cell imaging studies

Overall uptake of 2-NBDG (2-NBDG labeled versus unlabeled) was quantified for all 10 breast cell lines and then a new set of experiments was conducted for each anticancer or endocrine treatment (treated versus vehicle control). Each sample was defined as the average intensity of all cells within a single confocal image. The imaging field of view was 242 μm × 242 μm with 512 × 512 pixels per image. Two samples were acquired per plate. Sample sizes for each cell line included four, 2-NBDG labeled and four unlabeled plates. All 10 cell lines were tested in the unlabeled versus labeled experiments, and MDA-MB-435 and MDA-MB-468 cells were tested with anticancer agents (LND and α-Cinn) and MCF7 (ER+) and MDA-MB-435 (ER−) with endocrine therapy (tamoxifen).

2-NBDG uptake

Confocal microscopy imaging sessions were carried out 24 h after plating in the first experimental set that tested 2-NBDG uptake in all breast cell lines or after the treatment periods of 48 or 72 h, for the anticancer and endocrine therapies, respectively. The original cell media was removed from each dish, and cells were washed twice with PBS. Cells were labeled with either 100 μM 2-NBDG dissolved in glucose-free cell media, or glucose-free media alone for unlabeled cells, and incubated for 20 min. The media was then removed and the cells were washed 3 times with PBS and imaged. The concentration of 2-NBDG used was based on initial studies on two plates each of HMEC and MCF7 cell lines (data not shown). Cells, at 2-NBDG concentrations of 25, 50, 100, and 200 μM, were incubated with 2-NBDG for 20 min and were compared to equivalent unlabeled cells. Intracellular 2-NBDG fluorescence increased approximately linearly with concentration. However, at a concentration of 200 μM the fluorescence of most cells saturated the microscope detector. Therefore, a concentration in the middle of the tested range and equivalent to that used in previous cell studies [3], 100 μM, was chosen for subsequent studies. To determine the optimal time to measure 2-NBDG fluorescence (data not shown), two plates each of MCF7 and HMEC cells were tested at 10, 20 and 45 min. Fluorescence intensity was found to be significantly different after 20 min ($P < 0.05$) between 2-NBDG labeled and unlabeled cells and results matched previous studies at this time point [3].

Anticancer and endocrine treatments

A subset of cells (MDA-MB-435 and MDA-MB-468) was treated with the anticancer agents, LND, and α-cyano-hydroxycinnamate (α-Cinn). These cell lines were chosen since they both expressed HK I protein on a western blot ("Results"), and each cell line possesses unmethylated monocarboxylate transporter 1 (MCT1), which is the transporter that is blocked by α-Cinn [16]. Twenty-four hours after plating, cells were treated with 600 μM LND or 840 μM α-Cinn dissolved in dimethyl sulfoxide (DMSO) for 48 h [17]. The corresponding vehicle control was treated with DMSO only. Tam treatment was carried out at a concentration of 2 μM for 72 h, and the corresponding vehicle control was ethanol. G1 cell cycle arrest was determined via cell cycle analysis to occur in MCF7 cells after treatment with tam. After treatment, the cells were then labeled with 2-NBDG according to the protocol discussed and imaged at the settings described.

Data processing

Fluorescence intensity images were analyzed using NIH ImageJ software and analyzed with methods published previously [15]. Briefly, fluorescence intensity for each breast cell line was determined by manually segmenting each cell in the image and then computing the average fluorescence intensity for all cells in the image. Background intensity was subtracted and the resulting data normalized by a fluorescence calibration standard, which consisted of a fluorescent bead (FocalCheck Fluorescence Microscope Test Slide #2, Invitrogen, Carlsbad, CA, USA), measured daily to account for small changes in laser power. A total of $n = 8$ fields of view per cell line (two per sample per experimental arm) were imaged from which the average integrated fluorescence intensity per cell line was derived.

Western blots

Western blots were carried out according to standard procedures [18]. Briefly, after lysing the cells, resultant protein samples were heated to 95°C for 5 min and subjected to sodium dodecyl sulfate–polyacrylamide gel electrophoresis on 4–12% gradient 1-mm acrylamide gels, followed by transfer to polyvinylidene difluoride membranes for 1.5 h at 150 V with a NOVEX semi-transfer unit. Membranes were blocked for 1.5 h in Tris-buffered saline with 0.01% Tween 20, and incubated overnight with primary antibody: rabbit polyclonal GLUT 1 antibody or mouse monoclonal HK I antibody (Santa Barbara Biotech, California) in Tris-buffered saline with 0.01% Tween 20 with 10% bovine serum albumin. One hour incubation with horseradish peroxidase-conjugated anti-rabbit or mouse antibody, respectively, (Santa Barbara Biotech, California) followed. Blots were developed with an enhanced chemiluminescence kit (Amersham Pharmacia Biotech, Piscataway, NJ), and band intensity was quantified on the image by

manually circling signal area from blot background (Eastman Kodak Co., Rochester, NY). Signal was discriminated with a threshold determined from an 8-color rainbow look up table (signal was determined to be within the green–red coloration).

Statistics

All statistics were computed with JMP (SAS, Cary, NC, USA) software. ANOVAs and *t*-tests were completed with a Tukey–Kramer correction for multiple comparisons to determine statistical significance. Exact two-sided *P*-values were computed, and all $P < 0.05$ were considered significant. All correlations were calculated with a Pearson coefficient.

Results

A variety of breast cancer cells were tested in order to ensure that varying molecular phenotypes did not influence uptake of 2-NBDG. Estrogen receptor (ER), human growth receptor 2 (HER2), and progesterone receptor (PR) status are given for each cell line as reported by ATCC in Table 1.

Western blot results

Expression of GLUT 1 and HK I proteins was determined for all 10 cell lines with actin serving as an internal reference (Fig. 1). It is evident from the results that all malignant cell lines express measurable, but variable, GLUT 1 protein levels while the HMEC strain exhibits a negligible amount of GLUT 1 compared to its malignant counterparts. Interestingly, the other non-malignant epithelial line (MCF12) exhibited measurable levels of GLUT 1. HK I levels are widely variable across malignant cell lines. HMEC cells exhibit nominal levels of HK I when compared to malignant lines. The MCF12 line exhibited fairly high levels of HK I expression when compared to malignant cell lines. Furthermore, high GLUT 1 expression did not necessarily correspond to high HK I expression, as seen in the T47D cell line.

Table 1 Summary of cell lines tested and ER, HER2, and PR receptor status

Cell line	Type	ER	HER 2	PR
MCF12	Normal			
HMEC	Normal			
BT-474	Cancer	+	+	+
T47D	Cancer	+	−	+
MCF7	Cancer	+	−	+
MDA-MB-435	Cancer	−	−	−
BT-20	Cancer	−	−	−
MDA-MB-361	Cancer	+	+	−
MDA-MB-231	Cancer	−	−	−
MDA-MB-468	Cancer	−	−	−

2-NBDG uptake in cells

Figure 2 shows representative fluorescence intensity images of 2-NBDG labeled and unlabeled HMEC (normal) and MDA-MB-435 and MDA-MB-468 (cancer) cell lines. The two cancer cell lines shown were subsequently tested with both anticancer agents (LND and α-Cinn). All cell lines show similar diffusely distributed baseline fluorescence in the cytoplasm (as opposed to the nucleus), which is likely due to flavoproteins. HMEC does not show a significant increase in fluorescence after 2-NBDG labeling. Conversely, labeled breast cancer cell lines are significantly more fluorescent than unlabeled.

Figure 3 shows bar graphs of fluorescence intensity after 2-NBDG labeling for the 10 cell lines, grouped as normal mammary epithelial cells and breast cancer cells. Figure 3a shows mean calibrated fluorescence intensity stratified by cell line. Figure 3b shows Δ change in fluorescence intensity defined as: 2-NBDG labeled intensity − unlabeled fluorescence intensity. All cell lines exhibited significantly greater fluorescence intensity following 2-NBDG labeling ($P < 0.05$). As expected, all breast cancer cell lines had a significantly greater uptake of 2-NBDG than HMEC. MCF12 had an approximate 10-fold increase in 2-NBDG fluorescent intensity over the HMECs (Fig. 3a, b). Significant differences were observed between MCF12 and individual breast cancer cell lines (BT-20 and MDA-MB-468, specifically). When comparing the 2-NBDG fluorescence to the relative GLUT 1 and HK I protein expressions

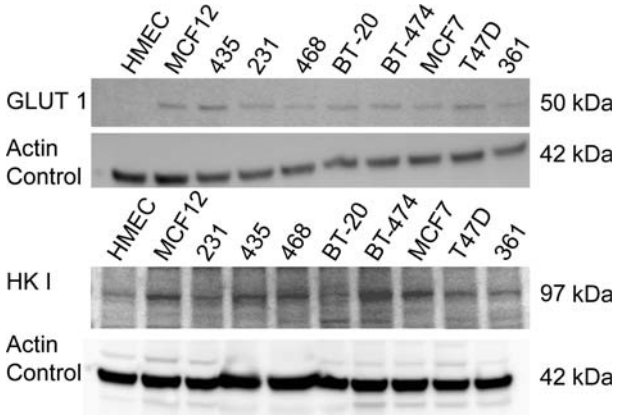

Fig. 1 Western blot analysis of GLUT 1 and HK I levels in 10 breast cancer cells

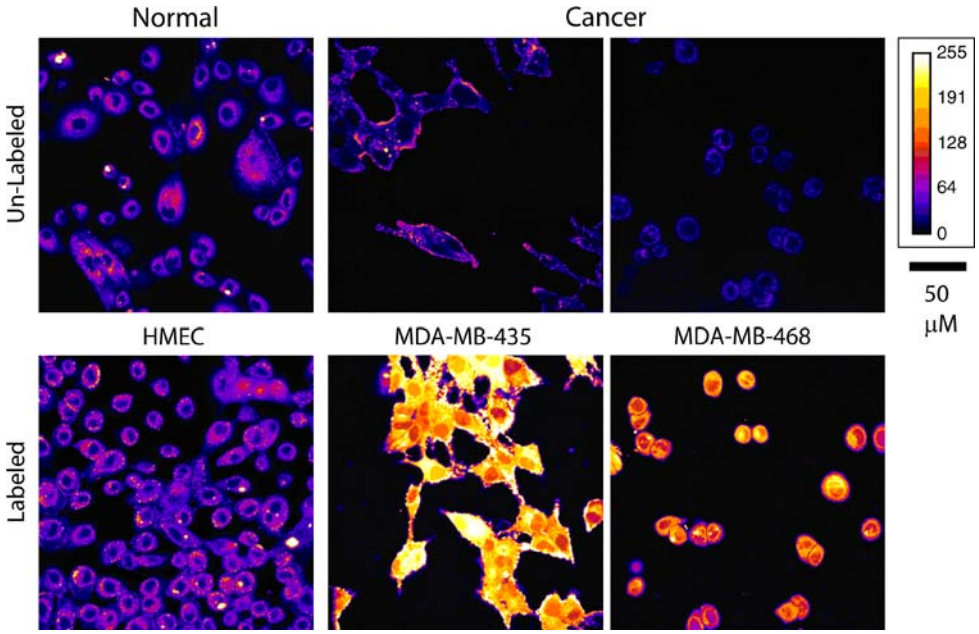

Fig. 2 Representative confocal fluorescence images of normal mammary epithelial and breast cancer cells 2-NBDG labeled and unlabeled. Excitation was at 488 nm, and emission was collected between 515 and 585 nm

shown in the western blot, no linear relationship was observed (Pearson correlation coefficient = 0.44; 0.50, respectively).

2-NBDG uptake after anticancer and endocrine treatments

All breast cancer cell lines demonstrated a significant increase in fluorescence intensity after 2-NBDG labeling. Therefore, a subset of two cell lines (MDA-MB-435 and MDA-MB-468) were treated with LND or α-Cinn to determine if a decrease or increase in glycolysis, respectively, could be measured with 2-NBDG. Figure 4 is a bar graph of the mean calibrated 2-NBDG fluorescence intensity of the two breast cancer cell lines treated with the agents (LND and α-Cinn) and vehicle controls.

Inhibition of HK I by LND demonstrated a significant inhibition of glucose uptake, as indicated by the decreased 2-NBDG fluorescence ($P < 0.05$). MDA-MB-468 demonstrated an approximate 50% decrease in 2-NBDG fluorescence intensity, whereas MDA-MB-435 fluorescence intensity only decreased by 15%. Inhibition of lactate-fueled respiration and subsequent increase in glycolysis via α-Cinn demonstrated the opposite trend. A significant increase in 2-NBDG uptake, as reflected by increased 2-NBDG fluorescence, was observed. MDA-MB-468 demonstrated a greater inhibition of 2-NBDG uptake after LND than MDA-MB-435, but increase in 2-NBDG fluorescence after α-Cinn treatment was similar ($P > 0.05$) between both cell lines. The increase in 2-NBDG fluorescence intensity was 20% and 25% for MDA-MB-468 and MDA-MB-435, respectively. It should be noted that the fluorescence intensity values shown in Fig. 4 cannot be directly compared with the results shown in Fig. 3 since the gain on the microscope was decreased to prevent 2-NBDG-labeled cell intensity from saturating the detector in the case of data collected for Fig. 4.

To ensure that 2-NBDG uptake could be influenced by indirect changes in cellular glycolysis and not only by direct inhibition or stimulation of glycolysis, tam-sensitive (MCF7 which are ER+) and -insensitive cells (MDA-MB-435 which are ER−) were treated with 2 μM tam. Rivenzon-Segal et al. had previously demonstrated GLUT 1 inhibition after 48 and 72 h of 2 μM of tam treatment in vitro [19]. GLUT 1 expression was measured following western blot analysis in tam-treated and vehicle control-treated MCF7 and MDA-MB-435 cell lines (Fig. 5a). Treated MCF7 cells showed a lower GLUT 1 expression as compared to control MCF7 cells, whereas the GLUT 1 expression of MDA-MB-435 cells was unchanged after treatment. The corresponding actin control is shown below GLUT 1. Accordingly, 2-NBDG uptake was significantly decreased in the treated MCF7 (tam-sensitive) cells over control MCF7 cells Fig. 5b. 2-NBDG uptake in MDA-MB-435 (tam-insensitive) cells did not change after treatment in Fig. 5b.

Discussion

This study demonstrates the ability to measure changes in glycolysis with the uptake of 2-NBDG via confocal fluorescence microscopy after anticancer and endocrine therapies. Our results showed that 2-NBDG accumulation in breast cell lines occurs in cells that express GLUT 1 regardless of receptor status. HMEC showed relatively

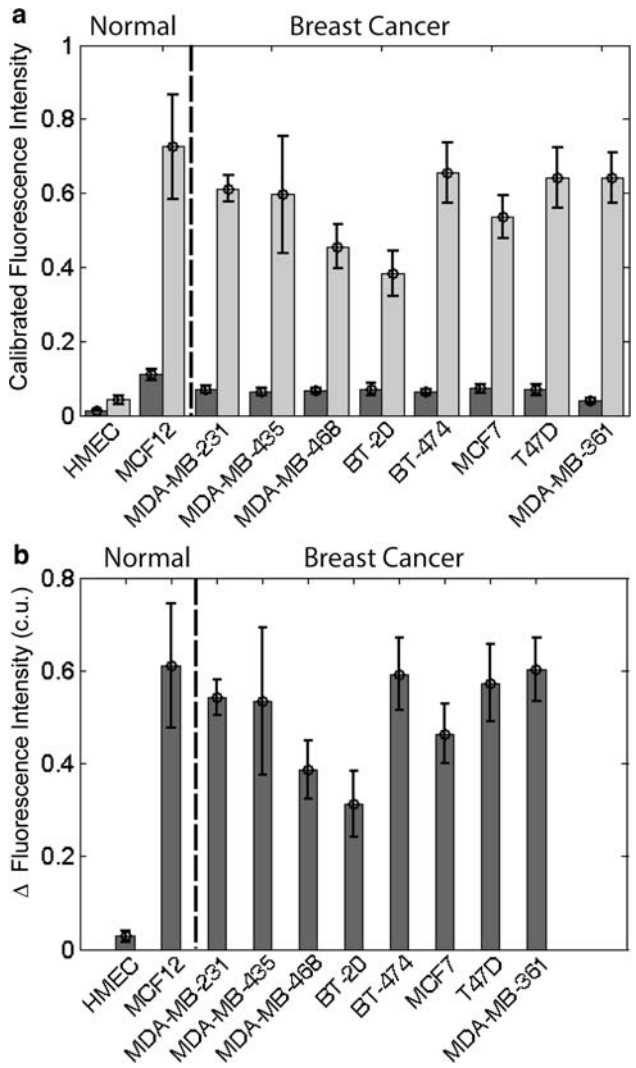

Fig. 3 **a** Mean calibrated fluorescence intensity values and standard deviation of all 10 tested cell lines. **b** Mean Δ change and standard deviation in fluorescence intensity. Note that both cell lines to the left of the *dashed line* in (**a**) and (**b**) are normal mammary epithelial cell lines, and cell lines to the right of the *dashed line* are breast cancer cell lines

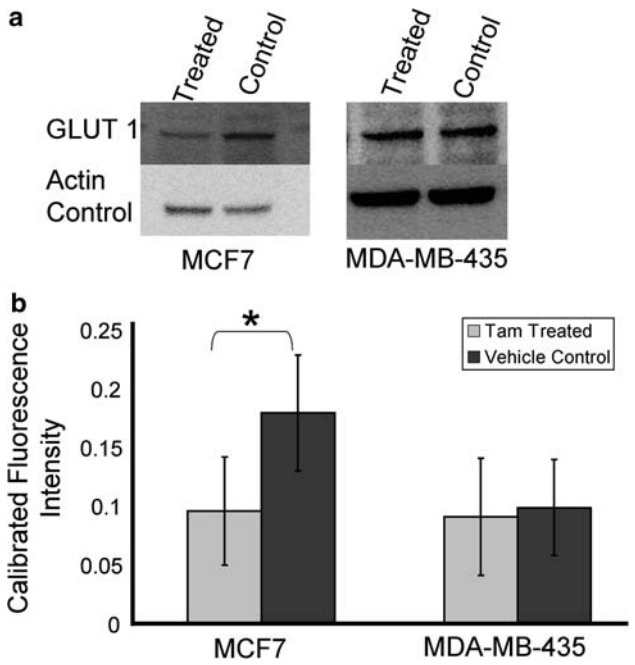

Fig. 5 **a** Western blot of GLUT 1 expression in treated and control MCF7 and MDA-MB-435 cell lines with corresponding actin controls below. **b** Calibrated mean fluorescence intensity values and standard deviation after treatment with tam in MCF7 and MDA-MB-435 cell lines (* denotes $P < 0.05$)

little 2-NBDG uptake, likely due to the very low levels of GLUT 1 expression. Previous in vitro studies carried out with 2-NBDG have shown that GLUT 1 influences competitive uptake using media with D-glucose, a GLUT 1 transporter specific glucose [13]. Our study quantified protein expression of GLUT 1 and HK I and demonstrated that HMEC expressed negligible GLUT 1 and had a significantly lower fluorescence intensity after 2-NBDG labeling. The normal MCF12 cell line, which expressed GLUT 1, took up a significant amount of 2-NBDG, as did all breast cancer cells. GLUT 1 is not typically overexpressed in normal mammary epithelium [11], and we

Fig. 4 **a** Calibrated mean fluorescence intensity values and standard deviation after treatment with LND in MDA-MB-468 and MDA-MB-435 cell lines. **b** Calibrated mean fluorescence intensity values and standard deviation after treatment with α-Cinn in MDA-MB-468 and MDA-MB-435 cell lines (* denotes $P < 0.05$)

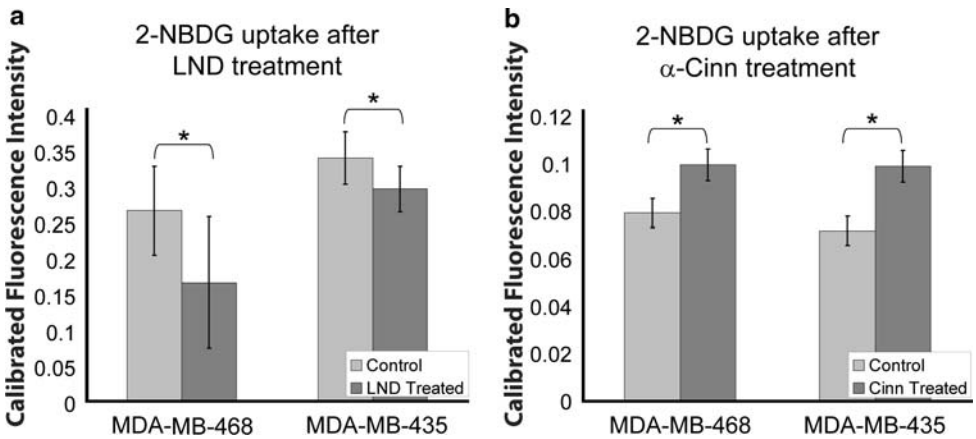

hypothesize GLUT 1 expression likely occurred during immortalization of MCF12.

A large panel of breast cancer cells was investigated to ensure that 2-NBDG could be used ubiquitously; all breast cancer cells demonstrated the ability to uptake 2-NBDG. However, variations in overall uptake could be seen between cell lines. It is believed to be due to differences in GLUT 1 and HK I expression and kinetics of 2-NBDG uptake in each cell line, which was not tested in this study. Only two cell lines were used to determine the optimal time point to examine 2-NBDG uptake. The uptake time of 20 min was chosen in order to be able to image the significant contrast between 2-NBDG labeled and unlabeled cells reasonably immediately.

Increasingly, drugs are being developed to target glycolysis [20]. To demonstrate 2-NBDG applicability to monitor breast cancer response to therapy, agents that directly inhibit and stimulate glycolysis were used on a subset of breast cancer cell lines. HK I protein, which is critical for glucose metabolism, was expressed in all cell lines. HK I has previously been demonstrated to be influential in the uptake of FDG [11]. GLUT 1 was expressed in all cells lines except in the HMECs. GLUT 1 has been previously shown to be over-expressed in breast cancer [21]. GLUT 1 and HK I did not directly correlate with the uptake of 2-NBDG in the breast cancer cell lines tested here. This could potentially be due to the fact that western blots are a measure of protein expression, and not the activity level. Also, several GLUT exist within the cell membranes that transport glucose, such as GLUT 2.

The importance of HK I was demonstrated by directly inhibiting it with the anticancer agent, LND [22]. LND decreased 2-NBDG uptake by inhibiting HK I. The greater inhibition in the uptake of 2-NBDG after LND treatment in MDA-MB-468 is believed to be due to the higher expression of HK I. However, from these studies it is difficult to explain specifically the basis for the differences in 2-NBDG uptake between the two cell lines. Possible sources for these differences could include overall kinetics of the pathways, protein activity within the cells, or dosage. Further experiments are needed to fully elucidate these differences. Nonetheless, a change in 2-NBDG uptake due to inhibition of HK has not been previously demonstrated. To ensure that inhibition of 2-NBDG uptake was not caused by the presence of the LND molecule, α-Cinn was also tested. α-Cinn has been previously shown in 2-NBDG studies to increase 2-NBDG uptake in neurons [16] and increase glucose use in SiHa cells [23], and therefore, α-Cinn should be able to demonstrate the stimulation of 2-NBDG uptake in breast cancer. The opposing trends in 2-NBDG uptake seen with treatment using α-Cinn also confirm that inhibition of LND is not caused by just the presence of the molecule and that 2-NBDG can be used to monitor stimulation or inhibition of glycolysis.

Vehicle controls shown in Fig. 4 have 200 μM DMSO and 160 μM DMSO added to media for the LND and α-Cinn treatments, respectively. 2-NBDG-labeled controls without DMSO were tested simultaneously and compared to DMSO-treated controls (not shown), and DMSO was shown to increase overall 2-NBDG fluorescence which reflects an increase in cell membrane permeability. Therefore, the vehicle controls treated with DMSO are shown in the Results (Fig. 4) to control for the effect of DMSO on 2-NBDG uptake in the LND and α-Cinn experiments.

Finally, MCF7, an ER+, and MDA-MB-435, an ER−, cell lines were treated with tam. Tam is a commonly used endocrine therapy that specifically targets ER [14] and is, therefore, a good candidate to demonstrate the applicability of 2-NBDG to breast cancer. Tam has been shown to decrease glycolysis [19, 24, 25] and inhibit GLUT 1 in vitro in tam-sensitive cells [19]. Previous studies have also shown a decrease in glycolysis after tam treatment by imaging FDG uptake [26, 27]. Uptake of 2-NBDG significantly decreased after treatment in MCF7 cells, but did not change in the MDA-MB-435 cell line. No response in the MDA-MB-435 cells showed the ability of 2-NBDG to monitor therapy response. An independent western blot analysis showed that GLUT 1 is important in the uptake of 2-NBDG in breast cancer.

The cellular origin of the MDA-MB-435 cell line has recently been questioned. Our group has previously reported similar uptake of aminolevulinic acid in MDA-MB-435, implying the cell line is similar to breast [15]. Although, it has previously been shown that the MDA-MB-435 has a gene expression profile consistent with M14 melanoma cells, recently Chambers [28] has argued that the MDA-MB-435 cell line is indeed of breast cancer origin. The argument stated that MDA-MB-435 originated from a female and the original M14 melanoma line was reported to be derived from a male patient [28]. The current M14 melanoma line stock does not contain a Y chromosome, which indicates that the M14 was most likely compromised [28]. In spite of the controversy surrounding the origin of the MDA-MB-435 cell line, the results from this study demonstrate concordance between MDA-MB-435 and the other breast cancer cell lines studied in terms of its uptake of 2-NBDG.

(2-(*N*-(7-nitrobenz-2-oxa-1,3-diazol-4-yl)amino)-2-deoxyglucose) uptake is a simple method to monitor changes in glycolysis and effectiveness of therapy. 2-NBDG can be further implemented in animal models to monitor the effects of drugs that affect glycolysis over time in vivo. Sheth et al. have successfully used an RFP murine dorsal window chamber model to show the overlap in 2-NBDG

uptake and RFP-labeled cancer cells [12]. Dorsal window chambers with 2-NBDG imaging would allow for longitudinal studies to examine effectiveness of therapies that perturb glycolysis. Other possibilities for pre-clinical monitoring of in vivo therapy could be to use spectroscopy or spectral imaging to monitor changes in 2-NBDG uptake in solid tumors. By utilizing the 2-NBDG molecule in conjunction with confocal, wide-field, or spectroscopy systems, glucose monitoring cost can be greatly reduced over other options such as microPET.

Acknowledgments The authors would like to acknowledge the support of the NIH Imaging Training Grant and DOD grant W81XWH-05-1-0363. Also, the Seewaldt lab has been especially helpful and is greatly appreciated for training SM in the use of molecular assays and for providing access to appropriate laboratory equipment.

References

1. Biersack HJ, Bender H, Palmedo H (2004) FDG-PET in monitoring therapy of breast cancer. Eur J Nucl Med Mol Imaging 31(Suppl 1):S112–S117
2. Nitin N, Carlson AL, Muldoon T, El-Naggar AK, Gillenwater A et al (2009) Molecular imaging of glucose uptake in oral neoplasia following topical application of fluorescently labeled deoxy-glucose. Int J Cancer 124:2634–2642
3. O'Neil RG, Wu L, Mullani N (2005) Uptake of a fluorescent deoxyglucose analog (2-NBDG) in tumor cells. Mol Imaging Biol 7:388–392
4. Livshits L, Caduff A, Talary MS, Lutz HU, Hayashi Y et al (2009) The role of GLUT1 in the sugar-induced dielectric response of human erythrocytes. J Phys Chem B 113:2212–2220
5. Meira DD, Marinho-Carvalho MM, Teixeira CA, Veiga VF, Da Poian AT et al (2005) Clotrimazole decreases human breast cancer cells viability through alterations in cytoskeleton-associated glycolytic enzymes. Mol Genet Metab 84:354–362
6. He Q, Xu RZ, Shkarin P, Pizzorno G, Lee-French CH et al (2003) Magnetic resonance spectroscopic imaging of tumor metabolic markers for cancer diagnosis, metabolic phenotyping, and characterization of tumor microenvironment. Dis Markers 19:69–94
7. Furman E, Rushkin E, Margalit R, Bendel P, Degani H (1992) Tamoxifen induced changes in MCF7 human breast cancer: in vitro and in vivo studies using nuclear magnetic resonance spectroscopy and imaging. J Steroid Biochem Mol Biol 43:189–195
8. Mestres P, Morguet A, Schmidt W, Kob A, Thedinga E (2006) A new method to assess drug sensitivity on breast tumor acute slices preparation. Ann N Y Acad Sci 1091:460–469
9. Ramanujan VK, Herman BA (2008) Nonlinear scaling analysis of glucose metabolism in normal and cancer cells. J Biomed Opt 13:031219
10. Yoshioka K, Saito M, Oh KB, Nemoto Y, Matsuoka H et al (1996) Intracellular fate of 2-NBDG, a fluorescent probe for glucose uptake activity, in *Escherichia coli* cells. Biosci Biotechnol Biochem 60:1899–1901
11. Bos R, van Der Hoeven JJ, van Der Wall E, van Der Groep P, van Diest PJ et al (2002) Biologic correlates of (18)fluorodeoxyglucose uptake in human breast cancer measured by positron emission tomography. J Clin Oncol 20:379–387
12. Sheth RA, Josephson L, Mahmood U (2009) Evaluation and clinically relevant applications of a fluorescent imaging analog to fluorodeoxyglucose positron emission tomography. J Biomed Opt 14:064014
13. Levi J, Cheng Z, Gheysens O, Patel M, Chan CT et al (2007) Fluorescent fructose derivatives for imaging breast cancer cells. Bioconjug Chem 18:628–634
14. Dietze EC, Troch MM, Bean GR, Heffner JB, Bowie ML et al (2004) Tamoxifen and tamoxifen ethyl bromide induce apoptosis in acutely damaged mammary epithelial cells through modulation of AKT activity. Oncogene 23:3851–3862
15. Millon SR, Ostrander JH, Yazdanfar S, Brown JQ, Bender JE et al (2010) Preferential accumulation of 5-aminolevulinic acid-induced protoporphyrin IX in breast cancer: a comprehensive study on six breast cell lines with varying phenotypes. J Biomed Opt 15:018002
16. Erlichman JS, Hewitt A, Damon TL, Hart M, Kurascz J et al (2008) Inhibition of monocarboxylate transporter 2 in the retrotrapezoid nucleus in rats: a test of the astrocyte-neuron lactate-shuttle hypothesis. J Neurosci 28:4888–4896
17. Floridi A, Paggi MG, D'Atri S, De Martino C, Marcante ML et al (1981) Effect of lonidamine on the energy metabolism of Ehrlich ascites tumor cells. Cancer Res 41:4661–4666
18. Pincheira R, Chen Q, Zhang JT (2001) Identification of a 170-kDa protein over-expressed in lung cancers. Br J Cancer 84:1520–1527
19. Rivenzon-Segal D, Boldin-Adamsky S, Seger D, Seger R, Degani H (2003) Glycolysis and glucose transporter 1 as markers of response to hormonal therapy in breast cancer. Int J Cancer 107:177–182
20. Pelicano H, Martin DS, Xu RH, Huang P (2006) Glycolysis inhibition for anticancer treatment. Oncogene 25:4633–4646
21. Brown RS, Goodman TM, Zasadny KR, Greenson JK, Wahl RL (2002) Expression of hexokinase II and Glut-1 in untreated human breast cancer. Nucl Med Biol 29:443–453
22. Di Cosimo S, Ferretti G, Papaldo P, Carlini P, Fabi A et al (2003) Lonidamine: efficacy and safety in clinical trials for the treatment of solid tumors. Drugs Today (Barc) 39:157–174
23. Sonveaux P, Vegran F, Schroeder T, Wergin MC, Verrax J et al (2008) Targeting lactate-fueled respiration selectively kills hypoxic tumor cells in mice. J Clin Invest 118:3930–3942
24. Rivenzon-Segal D, Margalit R, Degani H (2002) Glycolysis as a metabolic marker in orthotopic breast cancer, monitored by in vivo (13)C MRS. Am J Physiol Endocrinol Metab 283:E623–E630
25. Perumal SS, Shanthi P, Sachdanandam P (2005) Therapeutic effect of tamoxifen and energy-modulating vitamins on carbohydrate-metabolizing enzymes in breast cancer. Cancer Chemother Pharmacol 56:105–114
26. Monazzam A, Josephsson R, Blomqvist C, Carlsson J, Langstrom B et al (2007) Application of the multicellular tumour spheroid model to screen PET tracers for analysis of early response of chemotherapy in breast cancer. Breast Cancer Res 9:R45
27. Monazzam A, Razifar P, Simonsson M, Qvarnstrom F, Josephsson R et al (2006) Multicellular tumour spheroid as a model for evaluation of [18F]FDG as biomarker for breast cancer treatment monitoring. Cancer Cell Int 6:6
28. Chambers AF (2009) MDA-MB-435 and M14 cell lines: identical but not M14 melanoma? Cancer Res 69:5292–5293